

# Parallel robust relaxation algorithm for automatic stereo analysis

Kannappan Palaniappan, Jozsef Vass, and Xinhua Zhuang  
Multimedia Communications and Visualization Laboratory  
Department of Computer Engineering & Computer Science  
University of Missouri-Columbia  
Columbia, MO 65211, USA  
E-mail: {palani, vass, zhuang}@cecs.missouri.edu

## ABSTRACT

A parallel robust relaxation algorithm is proposed to improve the detection and correction of illegal disparities encountered in the automatic stereo analysis (ASA) algorithm. Outliers and noisy matches from correlation-based ASA matching are improved by relaxation labeling and robust statistical methods at each stage of the multiresolution coarse-to-fine analysis. A parallel version of the relaxation labeling algorithm has been implemented for the MasPar supercomputer. The performance scales quite linearly with the number of processing elements and scales better than linear with increasing work load. The algorithm is highly scalable both as the number of processors are increased for solving a fixed size problem and also as the size of the problem increases.

**Keywords:** parallel stereo, correlation matching, multiresolution algorithms, parallel relaxation labeling, robust estimation

## 1. INTRODUCTION

Cloud height measurement and cloud wind motion estimation from a time sequence of stereoscopic weather satellite imagery are very useful in many applications such as climate studies, radiation balance estimation, cloud model verification, cloud-height assignment and convective intensity estimation.<sup>1,2</sup> Stereoscopic measurement of cloud heights are essential because they provide basic information which is independent from other measurements; they could also assist in the accurate estimation of some physical parameters such as cloud-top temperature, cloud emittance, local lapse rate or optical thickness.

Several approaches for cloud height estimation have been tried with varying degree of success. Cloud shadow-based methods have the limitation of being applicable only during daytime primary over land where dark shadows can be matched with cloud features. CO2 slicing uses multispectral GOES VAS sounder to aid in operational cloud height assignment but is restricted since an estimate about the local lapse rate is required and currently involves a great deal of operator interaction.<sup>3</sup>

A major class of stereo analysis algorithms uses multiresolution analysis combined with a correlation-based measure of local similarity and adaptive window sizes. New techniques for handling mismatches and outliers due to noise, occlusion, reflectance change, specularities, transparency, motion, inexact modeling, etc. are needed to improve the accurate recovery of dense scene depth maps. Robust statistical methods have recently been applied to a variety of computer vision problems including motion estimation,<sup>4</sup> surface recovery from range data,<sup>5</sup> etc. Relaxation labeling algorithms are successfully applied to handle ambiguous matches by enforcing neighborhood smoothness constraints. In this paper, we develop a parallel robust relaxation algorithm that is applied after correlation-based matching to improve stereo-based extraction of depth or height. The parallel implementation of robust relaxation on the MasPar MP-2, a mesh connected architecture achieved nearly interactive performance.

The paper is organized as follows. The automatic stereo analysis algorithm is briefly described in Section 2. Relaxation labeling and its application to disparity refinement is presented in Section 3. The multistage robust algorithm is introduced in Section 4. Section 5 describes the proposed robust relaxation robust algorithm, and the last section gives conclusions and further research directions.

## 2. AUTOMATIC STEREO ANALYSIS ALGORITHM

The goal of the Automatic Stereo Analysis (ASA) algorithm, which was previously developed and implemented by the authors on a massively parallel supercomputer (MasPar) at NASA/Goddard Space Flight Center, is to find correspondence between the reference and test satellite-based stereo image pair which is used to estimate the disparity or depth map. It follows the hierarchical approach first proposed by Marr and Poggio.<sup>6</sup> The approach starts with low resolution and increases to higher resolution. However, instead of generating and matching images at several levels, multiresolution matching is simulated by varying the size of the template windows (matching blocks). The ASA algorithm belongs to the class of correlation-based stereo analysis algorithms, i.e., matching is based on maximizing the normalized cross-correlation coefficient for a template centered around a pixel of interest in the reference image. Then, the disparity map is used to warp the test image so that searching at the next finer level can be done with a smaller template. Illegal disparities (outliers) or mismatches are detected by constraining the acceptable value for the local disparity gradient and replacing illegal disparities with an interpolated value using a second order diffusion model. The process iterates until the changes in the disparity is inferior to a given threshold, or the maximum number of iterations is exhausted.

The parallel ASA enabled interactive testing and evaluation of the computationally expensive ASA algorithm on large datasets such as remote sensing imagery. The main steps of the parallel ASA algorithm implemented on the MasPar supercomputer are summarized in the followings.<sup>7,8</sup> Suppose that the stereo image pair consists of a reference image  $f_r$  and a test image  $f_t$ .

**Step 1. Preprocessing of images.** Due to complex and time-varying sensor geometries the stereo pairs are reprojected or rectified so that epipolar lines are horizontal. The sensor data may need to be radiometrically corrected and enhanced so that the reference and test data have histograms of roughly the same shape. This is accomplished by rescaling the pixel brightness in both the reference and test images to the full range of values.

**Step 2. Automatic template size search.** Determine the starting resolution (coarsest template size) for initial matching using the local gradient of the weighted entropy and gradient of the standard deviation measures.

**Step 3. Initialize disparities.** If available a prior disparity estimates from other sources can be incorporated (i.e., from infrared measurements) to constrain matching.

**Step 4. Warp test image.** The original test image is warped using the cumulative disparities estimated up to the current scale (iteration). The warped image values are obtained by resampling the test image using bilinear interpolation.

**Step 5. Determine image matches.** For each reference image pixel, a match score is computed between a template centered at the pixel and neighborhoods within a search area in the test image. At finer scales the template sizes and search areas are reduced to extract smaller scale features. The region-based measure used for stereo matching is a normalized correlation coefficient,

$$R(k, l) = \frac{\sum_{x,y} (f_r(x, y) - \bar{f}_r(x, y)) (f_t(x - k, y - l) - \bar{f}_t)}{\sqrt{\left(\sum_{x,y} (f_r(x, y) - \bar{f}_r(x, y))\right)^2 \left(\sum_{x,y} (f_t(x - k, y - l) - \bar{f}_t)\right)^2}},$$

where  $f_r(x, y)$  and  $f_t(x, y)$  correspond to template pixels within the reference and test images, respectively. The values  $\bar{f}_r$  and  $\bar{f}_t$  are the corresponding mean values. For each pixel in the reference image, the match scores for all pixels in the neighborhood within the search area are computed. The pixel at the center of the search template with the highest correlation match score is selected as corresponding candidate pixel and the vector  $(k, l)$  gives the estimate of the disparity,

$$\begin{pmatrix} k \\ l \end{pmatrix} = \arg \max R(k, l).$$

**Step 6. Detect illegal disparities.** Local continuity of surfaces is used by constraining the disparity gradient to mark outlier disparities for correction. A disparity gradient threshold is used to constrain the maximum local slope.

**Step 7. Interpolate over outlier disparities.** Interpolation using local neighboring disparities is done using an iterative second order diffusion model at positions where the maximum disparity gradient is exceeded.

**Step 8. Smooth disparities.** Smoothing of the disparity field can be done to mitigate noise before image warping and matching at the next finer-scale of the hierarchy. Smoothing is performed by averaging over a neighborhood of size proportional to the template size.

**Step 9.** If the disparity change is small, or the number of iterations is exhausted then terminate; otherwise go to **Step 4.**

The multiresolution correlation-based approach developed in the ASA algorithm is now being applied in a variety of fields. Our testing has shown that the ASA algorithm has good performance for a variety of stereo cloud image pairs from remote sensing satellites.<sup>9,10</sup>

### 3. RELAXATION LABELING

Launched by Rosenfeld *et al.* in 1976<sup>11</sup> relaxation labeling has found its way in various applications.<sup>12,13</sup> A consistent labeling problem<sup>14</sup> has many units (each pixel in the image) each of which has an unknown true label (disparity). There are  $N$  units  $U_1, \dots, U_N$  and  $M$  labels  $L_1, \dots, L_M$ . Each unit has a labeling distribution, i.e., a set of numbers  $p(i) = [p_1(i), \dots, p_M(i)]^T$  associated with the probability of the corresponding labels at unit  $U_i$ . The correlation matching algorithm described above will be used to generate candidates with initial probabilities for each unit. Then the probabilities are updated to give an unambiguous labeling.

Consider two neighboring units  $U_i$  and  $U_h$  and their respective labels  $L_j$  and  $L_k$ . Then let a real number termed *compatibility coefficient*  $r(i, j; h, k)$  represent how label  $L_k$  at unit  $U_h$  influences the label  $L_j$  at unit  $U_i$ . If the unit  $U_h$  having the label  $L_k$  lends a high support to the unit  $U_i$  having the label  $L_j$ , then  $r(i, j; h, k)$  should be large. If the constraints are such that the unit  $U_h$  having the label  $L_k$  means that the label  $L_j$  at the unit  $U_i$  is highly unlikely, then  $r(i, j; h, k)$  should be small.

In the developed algorithm, each pixel is a unit. The label associated with each pixel is the corresponding disparity. The compatibility coefficients has two parts, i.e., the difference between labels weighted by the distance between the units,

$$r(i, j; h, k) = \alpha(i, j; h, k)\beta(i, h).$$

In this research, the difference between labels is calculated by

$$\alpha(i, j; h, k) = \left( 1 - \frac{|(L_j \text{ at } U_i) - (L_k \text{ at } U_h)|}{\text{Maximum disparity range}} \right).$$

It is clear from the above equation, that large discrepancy between labels results in low compatibility. If the two disparities are similar, then the compatibility  $\alpha(i, j; h, k)$  is high, i.e., the two units are supporting each other. Note that  $\alpha(i, j; h, k)$  is in the range of  $[0, 1]$ ;

The label difference  $\alpha(i, j; h, k)$  is then weighted by the distance between the corresponding units calculated by using

$$\beta(i, h) = \exp\left(\frac{|U_i - U_h|}{d_{max}}\right),$$

where  $d_{max}$  is a normalizing variable. In general,  $d_{max}$  is a function of position. At motion discontinuity,  $d_{max}$  should be small, so neighboring pixels are only loosely related. However, in large smooth areas, it is desirable to increase the value of  $d_{max}$ . Increasing  $d_{max}$  increases the computational complexity, since larger neighborhood are involved. For simplicity, in our implementation,  $d_{max}$  is constant,  $d_{max} = 20$ . Note, that similarly to  $\alpha(i, j; h, k)$ ,  $\beta(i, h)$  is in the range of  $[0, 1]$ , thus the compatibility coefficient  $r(i, j; h, k)$  is also in the range of  $[0, 1]$ .

Define the *support* on unit  $U_i$  having label  $L_j$  from unit  $U_h$  having the labeling distribution  $p(h)$  by

$$q(i, j) = \sum_{k=1}^M r(i, j; h, k)p_k(h),$$

where  $M$  is the number of labels, and  $i = 1, \dots, N$  and  $j = 1, \dots, M$ .

Then at the  $(l + 1)$ th iteration the probabilities are updated according to

$$p_j^{l+1}(i) = \frac{p_j^l(i) (1 + q(i, j))}{\sum_{r=1}^M p_r^l(i) (1 + q(i, r))},$$

where the denominator used to normalize the sum of probabilities to 1 and  $l$  denoted the number of iteration.

Usually, the relaxation labeling process is terminated when the absolute probability difference between consecutive iterations is inferior to a specified threshold,

$$\frac{1}{M} \frac{1}{N} \sum_{i=1}^N \sum_{j=1}^M |p_j^{l+1}(i) - p_j^l(i)|.$$

### 3.1. Parallel implementation issues

The parallel version of the above relaxation labeling algorithm was implemented on the MasPar MP-2 supercomputer. The MasPar MP-2 at NASA Goddard Space Flight Center is a single instruction, multiple data (SIMD) massively parallel machine with 16384 processor elements (PE) arranged in a rectangular mesh of size  $128 \times 128$ . Each PE is a 32-bit RISC processor with a separate floating point unit with 40 user accessible registers and 64 kilobytes of memory. Since we use images with dimensions of  $512 \times 512$ ,  $4 \times 4$  pixels are handled with each PE. The 2-D array of PE-s are interconnected in an 8-way nearest neighbor X-net mesh. Although, the PE-s can also communicate via a multistage circuit-switched interconnection network (Global Router), we use direct communication via X-nets due to the much higher available bandwidth. The parallel implementation of the relaxation labeling algorithm can be further optimized in terms of memory usage by using only one array for storing and updating the label probabilities since coherent read and write operation are guaranteed.

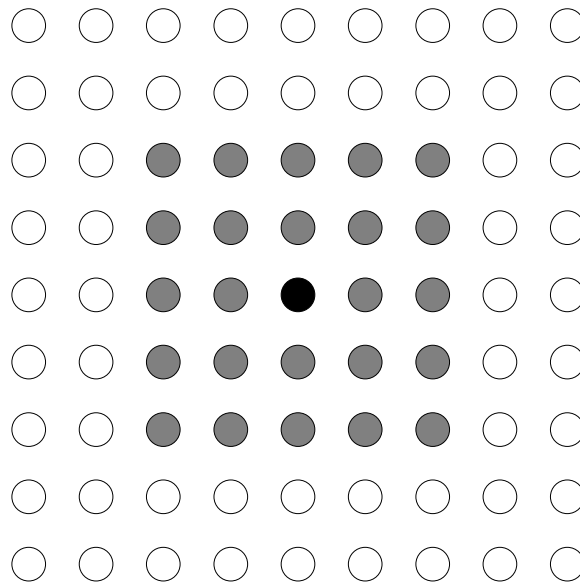


**Figure 1.** Candidate neighborhood in relaxation labeling algorithm.

The performance of parallel relaxation labeling algorithm is mainly depends of the neighborhood used to calculate the compatibility coefficients. The size of the neighborhood also influences the interaction of pixels with each other. In our experiments, the neighborhood ranges from  $3 \times 3$  pixels to  $11 \times 11$  pixels. A  $5 \times 5$  neighborhood is shown in Fig. 1.

The efficiency of our parallel implementation is measured by *speed-up* and *scalability*. Speed-up  $S_p(n)$  is measured by the total execution time at constant workload with  $n$  number of PEs. Speed-up measures the rate of decrease in execution time, as a function of machine size, for a fixed problem size,

$$S_p(n) = \frac{t_1}{t_n} = \frac{\text{problem execution time on one processor}}{\text{problem execution time on } n \text{ processors}}.$$

Experiments were carried out on the MasPar MP-2 with the number of PEs ranging from 1024 to 16384. The speed-up curve for the parallel relaxation labeling algorithm is shown in Fig. 2, using  $t_{1024}$  as the reference instead of  $t_1$ , due to the minimum PE configuration and the 64 Kbyte per PE constraint of the MasPar.

Scalability  $S_c(n)$ , is a dimensionless ratio of execution times, measured by increasing the workload when the number of PEs is increased at the same rate,

$$S_c(n) = \frac{T_{n \times w}}{T_w} = \frac{\text{execution time for application doing } n \times w \text{ work on } n \text{ processors}}{\text{execution time doing } w \text{ work on a single processor}}.$$

We measure the scalability for two different types of work: with the number of candidates being constant and the neighborhood for relaxation labeling being increased, and with the neighborhood being constant and the number of candidates being increased as shown in Fig. 3. The speed-up performance of the parallel implementation scales nearly linearly with the number of processing elements and scales better than ideal,  $S_c(n) < 1.0$ , with increasing work load as the number of processors is increased from 1024 to 16384.

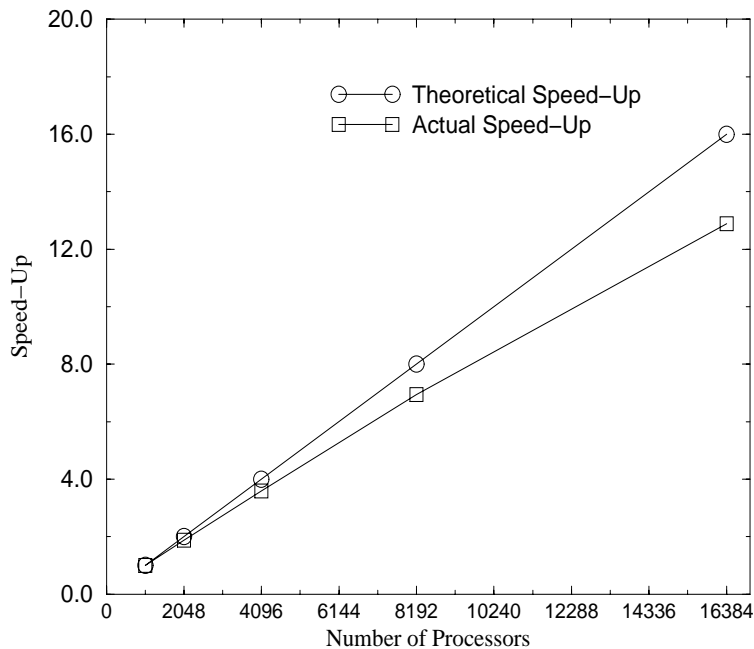


**Figure 2.** Speed-up of parallel relaxation labeling algorithm on MasPar.

Fig. 4a shows the result of the correlation matching algorithm after selecting the most probable disparities. Numerous bad matches are visible. Applying only one step of relaxation labeling greatly improves the results as shown in Fig. 4b. By using neighborhood constraint, large portion of the bad matches were corrected. We have also found, that several iterations of relaxation labeling does not necessarily improve the result in terms of warped disparity error. The reason for this is that relaxation labeling smooth the disparity function, which might not be appropriate all the time.

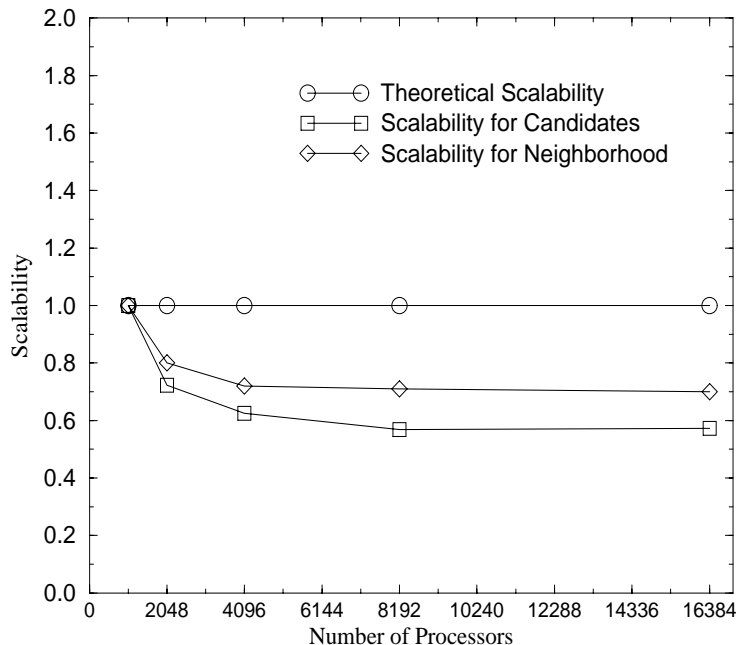


**Figure 3.** Scalability of parallel relaxation labeling algorithm on MasPar.

#### 4. ROBUST ESTIMATION

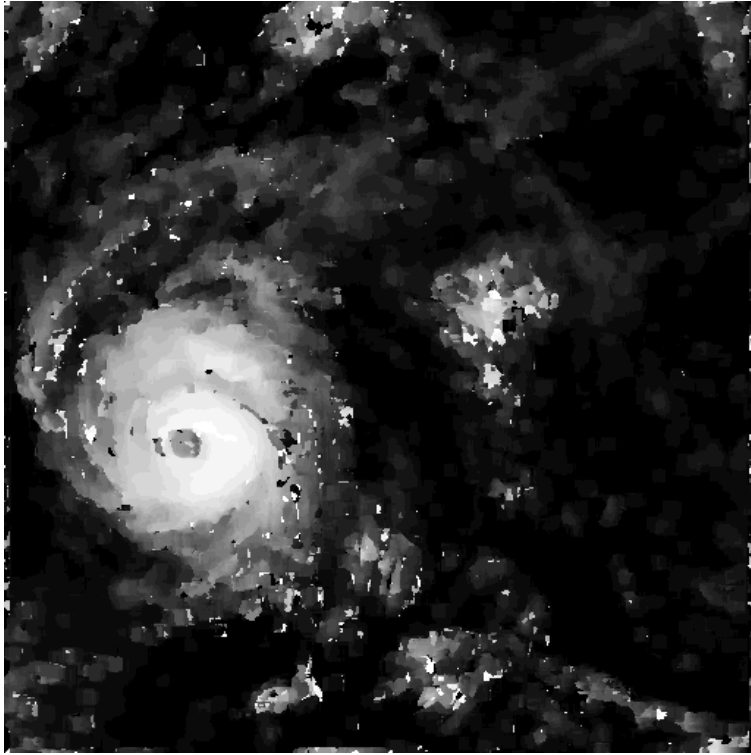
Multistage adaptive robust (MAR)<sup>15</sup> algorithm was developed to improve the result of the ASA algorithm.<sup>16</sup> As seen, in the ASA algorithm the disparity is assumed to be translational. MAR enhances ASA by modeling the disparity by using affine transformation. When the matching patch contains depth boundaries, shape distortion or occlusion, it can be considered as multi-structured possibly consisting of multiple patches, each of which contains a portion of the original data set supporting a distinct matching model. Thus the matching error are no longer Gaussian distributed under any set of model parameters; instead, they form a mixture of Gaussian distributions and possibly outliers under appropriate sets of (unknown) model parameters.

The MAR algorithm contains three stages. First, the affine parameters are estimated traditional, non-linear least-square estimator by using gradient-descent method. If the disparity error is larger than a predefined value, than the least-square estimation is considered unreliable, and the disparity will be reestimated at the second stage by using bi-weight estimator. Typically, the bi-weight estimator can tolerate 30–40% of outliers. If the bi-weight estimator fails (large disparity error), then the MF estimator<sup>15</sup> is used as a generic robust estimator capable of handling multi-structure data sets. The MF estimator is capable of estimating a valid model from a mixture data set without much influenced by the irrelevant data and outliers.

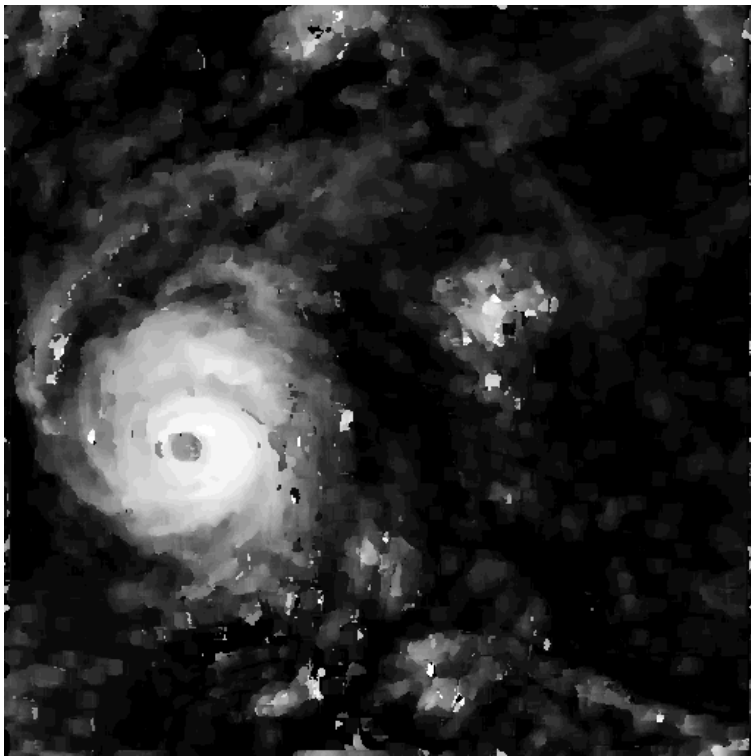
All the above three estimation methods require initial estimates of the disparities which is provided by the ASA algorithm. Extensive performance evaluation shows that MAR algorithm reduces the absolute warped error by about 20% when compared to the ASA algorithm.

#### 5. PROPOSED ALGORITHM

As seen, the ASA algorithm determines the disparity by maximizing the correlation coefficients. However, by using relaxation labeling, no decision is made based on solely the correlation coefficients as in ASA; several candidates with high correlation coefficients are kept for further evaluation. The underlying assumption is that the true disparity vector, if exists, must be close to one of the candidates. Then, the initial estimates are refined by using robust



(a)



(b)

**Figure 4.** (a) Result of correlation matching. (b) Result after one iteration of relaxation labeling.

estimation techniques similar that of in the MAR algorithm. After this step, the true disparity, if exists, would be found by refining the initial disparity vector. Finally, relaxation labeling is applied on the refined disparities to obtain a consistent disparity field.

The main steps of the correlation-relaxation-robust algorithm is summarized as follows.

**Step 1.** Preprocessing of images.

**Step 2.** Automatic template size search.

**Step 3.** Initialize disparities.

**Step 4.** Warp test image.

**Step 5.** Candidate generation by correlation matching.

**Step 6.** Refinement of disparities by using affine disparity model and robust algorithm.

**Step 7.** Relaxation labeling to resolve ambiguity among matches.

**Step 8.** If more refinement is required then go to **Step 4**.

## 6. CONCLUSIONS AND FURTHER RESEARCH DIRECTIONS

In the paper, a robust relaxation algorithm is developed and tested for automatic disparity field estimation from satellite stereo image pairs. Robust estimation methods are used to combat the effect of outliers combined with relaxation labeling to obtain consistent disparity fields.

Further research directions include 1) improving the performance of relaxation labeling. A possible problem with relaxation labeling is the smoothness assumption, which might not be satisfied for certain image regions such as cloud edges, shadowing, occlusion, and multiple transparent clouds. In this case, relaxation labeling causes undesirable smoothing effects. Thus by segmenting the image into matchable and non-matchable regions and constructing a so-called relaxation-mask, relaxation labeling can only be applied on the matchable regions, non-matchable regions can be interpolated by using the heat equation. 2) Improving the speed of relaxation labeling by using e.g., simplex-like algorithm.<sup>17</sup>

## 7. ACKNOWLEDGMENT

This research was partially supported by several National Aeronautics and Space Administration (NASA) equipment and research grants including AISRP NRA-93-OSSA-09, NRA-94-MTPE-02, RTOP 578-12-06-20 (IISS), NAG 5-3900, NRA 94-OSS-16, and NRA 97-MTPE-05. J. Vass was supported by the NASA Visiting Student Enrichment Program internship at Goddard Space Flight Center (GSFC) during summer 1996, when the relaxation algorithm was implemented on the MasPar. Datasets were obtained from Dr. A.F. Hasler at NASA GSFC Lab. for Atmospheres and the GOES Project Office.

## REFERENCES

1. A.F. Hasler and K.M. Morris, "Hurricane structure and wind fields from stereoscopic and infrared satellite observations and radar data," *Journal of Applied Meteorology*, vol. 25, no. 6, pp. 709-727, June 1986.
2. A.F. Hasler, "Stereographic observations from satellites: An important new tool for the atmospheric sciences," *Bulletin of the American Meteorological Society*, vol. 62, pp. 194-212, 1981.
3. R.T. Merril, W.P. Menzel, W. Baker, J. Lynch, and E. Legg, "A report on the recent demonstration of NOAA's upgraded capability to derive cloud motion setellite winds," *Bulletin of the American Meteorological Society*, vol. 72, pp. 372-376, 1991.
4. Y. Huang, K. Palaniappan, X. Zhuang, and J. Cavanaugh, "Optic flow field segmentation and motion estimation using a robust genetic partitioning algorithm," *IEEE Transactions on Pattern Analysis and Machine Intelligence*, vol. 17, no. 12, pp. 1177-1190, Dec. 1995.

5. C.V. Stuart, "A new robust operator for computer vision: Application to range data," in *Proceedings of IEEE International Conference on Computer Vision and Pattern Recognition*, 1994, pp. 167–173.
6. D. Marr and T. Poggio, "A computational theory of human stereo vision," *Proceedings of Royal Society London*, pp. 301–328, 1979.
7. K. Palaniappan, C. Kambhamettu, F. Hasler, and D. Goldgof, "Structure and semi-fluid motion analysis of stereoscopic satellite images for cloud tracking," in *Proceedings of International Conference on Computer Vision*, 1995, pp. 659–665.
8. K. Palaniappan, M. Faisal, C. Kambhamettu, and F. Hasler, "Implementation of an automatic semi-fluid motion analysis algorithm on a massively parallel computer," in *Proceedings of International Parallel Processing Symposium*, 1996, pp. 864–872.
9. H.K. Ramapriyan, J.P. Strong, Y. Hung, and C.W. Murray, "Automated matching of pairs of SIR-B images for elevation mapping," *IEEE Transactions on Geoscience and Remote Sensing*, vol. 24, no. 4, pp. 462–472, July 1986.
10. A.F. Hasler, J. Strong, R.H. Woodward, and H. Pierce, "Automatic analysis of stereoscopic satellite image pairs for determination of cloud-top height structure," *Journal of Applied Meteorology*, vol. 30, no. 8, pp. 257–281, Aug. 1991.
11. A. Rosenfeld, R.A. Hummel, and W. Zucker, "Scene labeling by relaxation operation," *IEEE Transactions on Systems, Man, and Cybernetics*, vol. 6, no. 6, pp. 420–433, June 1976.
12. Q.X. Wu, "A correlation-relaxation framework for computing optical flow – template matching from a new perspective," *IEEE Transactions on Pattern Analysis and Machine Intelligence*, vol. 17, no. 8, pp. 843–853, Sept. 1995.
13. Q.X. Wu and D. Pairman, "A relaxation labeling technique for computing sea surface velocities from sea surface temperatures," *IEEE Transactions on Geoscience and Remote Sensing*, vol. 33, no. 1, pp. 216–220, Jan. 1995.
14. R.A. Hummel and S.W. Zucker, "On the foundation of relaxation labeling processes," *IEEE Transactions on Pattern Analysis and Machine Intelligence*, vol. 5, no. 3, pp. 267–287, May 1983.
15. X. Zhuang, T. Wang, and P. Zhang, "A highly robust estimator through partially likelihood function modeling and its application in computer vision," *IEEE Transactions on Pattern Analysis and Machine Intelligence*, vol. 14, no. 1, pp. 19–35, Jan. 1992.
16. K. Palaniappan, Y. Huang, X. Zhuang, and F. Hasler, "Robust stereo analysis," in *Proceedings of IEEE International Symposium on Computer Vision*, 1995, pp. 175–181.
17. X. Zhuang, R.M. Haralick, and H. Joo, "A simplex-like algorithm for relaxation labeling process," *IEEE Transactions on Pattern Analysis and Machine Intelligence*, vol. 11, no. 12, pp. 1316–1321, Dec. 1989.